

# Magnetism and superconductivity in Eu<sub>0.2</sub>Sr<sub>0.8</sub>(Fe<sub>0.86</sub>Co<sub>0.14</sub>)<sub>2</sub>As<sub>2</sub> probed by <sup>75</sup>As NMR

R Sarkar <sup>‡</sup>, <sup>†</sup> R Nath, P Khuntia, <sup>§</sup> H S Jeevan, <sup>§</sup> P Gegenwart  
and M Baenitz

Max-Planck Institute for Chemical Physics of Solids, 01187 Dresden, Germany

<sup>†</sup>School of Physics, Indian Institute of Science Education and Research,  
Thiruvananthapuram-695016, India

<sup>§</sup>I. Physik. Institut, Georg-August-Universität Göttingen, 37077 Göttingen, Germany

E-mail: rajibsarkarsinp@gmail.com, rajib.sarkar@cpfs.mpg.de

## Abstract.

We report bulk superconductivity (SC) in Eu<sub>0.2</sub>Sr<sub>0.8</sub>(Fe<sub>0.86</sub>Co<sub>0.14</sub>)<sub>2</sub>As<sub>2</sub> single crystals by means of electrical resistivity, magnetic susceptibility, and specific heat measurements with  $T_c \simeq 20$  K with an antiferromagnetic (AFM) ordering of Eu<sup>2+</sup> moments at  $T_N \simeq 2.0$  K in zero field. <sup>75</sup>As NMR experiments have been performed in the two external field directions (H||*ab*) and (H||*c*). <sup>75</sup>As-NMR spectra are analyzed in terms of first order quadrupolar interaction. Spin-lattice relaxation rates ( $1/T_1$ ) follow a  $T^3$  law in the temperature range 4.2-15 K. There is no signature of Hebel-Slichter coherence peak just below the SC transition indicating a non *s*-wave or *s*<sub>±</sub> type of superconductivity. The increase of  $1/T_1T$  with lowering the temperature in the range 160-18 K following  $\frac{C}{T+\theta}$  law reflecting 2D AFM spin fluctuations.

<sup>‡</sup> Author to whom all correspondence should be made.

## 1. Introduction

The recent discovery of superconductivity (SC) in Fe based pnictides has attracted considerable attention in the condensed matter physics community to understand the microscopic origin of the SC and its relation to the Fe based magnetism [1, 2, 3, 4, 5, 6, 7]. In this diverse branch of pnictides one family of materials  $\text{AFe}_2\text{As}_2$  ( $\text{A}=\text{Ca}, \text{Sr}, \text{Ba}, \text{Eu}$ ) (abbreviated as 122 series) with the crystal structure of  $\text{ThCr}_2\text{Si}_2$  type exhibits the SC with the transition temperatures  $T_C$ 's as high as 38 K [8, 9, 10]. Interestingly in this 122 family,  $\text{EuFe}_2\text{As}_2$  is the only member which has a rare earth moment  $\text{Eu}^{2+}$  ( $S=7/2$ ) corresponding to a theoretical effective moment of  $7.94 \mu_B$ . Here the antiferromagnetic (AFM) ordering of  $\text{Eu}^{2+}$  moments take place at 19 K and Fe order AFM (SDW type) at 190 K, which is the highest reported SDW transition temperature among the pnictide family [11, 12, 14]. The SC could be found in this compound with the suppression of the Fe ordering by the K substitution (hole doping) at the  $\text{Eu}^{2+}$  site with  $T_C$ 's upto 32 K [8]. In addition to that SC has been observed in chemically pressurized  $\text{EuFe}_2(\text{As}_{1-x}\text{P}_x)_2$  alloys accompanied by the  $\text{Eu}^{2+}$  ordering [15, 16].

In contrast to the other 122 systems, in  $\text{EuFe}_2\text{As}_2$ , on suppression of the AF order of iron with pressure or Co doping, the onset of SC was observed, however seem to be hindered to reach zero resistivity because of the magnetic ordering of  $\text{Eu}^{2+}$  [17, 18, 19]. Nevertheless by substituting 80 % Sr at the  $\text{Eu}^{2+}$  and optimal Co doping at the Fe site one can suppress the AFM ordering of  $\text{Eu}^{2+}$ , and Fe SDW ordering, respectively. Eventually, SC with the  $T_C$ 's 20 K is being observed [20]. Apart from the SC, this system could be also interesting to study the interplay between Fe-3d and Eu-4f magnetism. Especially if there is any coupling present between the two subsystem (Fe-3d and Eu-4f). Here it is worth to mention the  $\text{Eu}^{2+}$  ordering at 19 K in  $\text{EuFe}_2\text{As}_2$  perhaps makes this system much more interesting, because this could additionally opens up the opportunity to clarify the mechanism of the interplay between the 3d and 4f magnetism and also the influence of  $\text{Eu}^{2+}$  magnetism on the SC. It has been already suggested from different experiments that there is coupling between the localized  $\text{Eu}^{2+}$  moments and the conduction electrons of the two dimensional  $\text{Fe}_2\text{As}_2$  layers [21, 22, 23].

In this paper we present the electrical resistivity ( $\rho$ ), magnetic susceptibility ( $\chi$ ), and heat capacity ( $C_p$ ) measurements on superconducting  $\text{Eu}_{0.2}\text{Sr}_{0.8}(\text{Fe}_{0.86}\text{Co}_{0.14})_2\text{As}_2$  (abbreviated as ESFCA) single crystal. All these experiments are complemented by  $^{75}\text{As}$  NMR measurements to shed light on the microscopic properties. Here it is worth emphasizing numerous NMR investigations have been done to understand the microscopic mechanism of the 122 (Ca, Sr, Ba) based superconductors, for instance [Ref[24, 25, 26, 27, 28]]. However, to the best of our knowledge there is only one reported NMR investigation on this Eu based 122 system, namely  $\text{EuFe}_{1.9}\text{Co}_{0.1}\text{As}_2$ . Guguchia et. al. have suggested, there is strong coupling between the  $\text{Eu}^{2+}$  moments and the  $\text{Fe}_{1.9}\text{Co}_{0.1}\text{As}_2$  layers [29]. However, authors have not focused on the superconducting region. Therefore still there is a scope to investigate the Eu based pnictides superconductors to simplify the superconducting mechanism and the possible

role of Eu magnetism on the superconducting state. We believe our present investigations will answer these questions adequately.

## 2. Experimental details

Single crystals of  $\text{Eu}_{0.2}\text{Sr}_{0.8}\text{Fe}_2\text{As}_2$  and ESFCA were synthesized using Sn flux method. Nominal stoichiometric amounts (0.8:0.2:2:2 for  $\text{Sr}_{0.8}\text{Eu}_{0.2}\text{Fe}_2\text{As}_2$  and 0.8:0.2:1.4:0.6:2 for ESFCA) of the respective starting elements were taken in alumina crucibles, sealed in a quartz tube under Ar atmosphere. The batches were heated to 1300 °C at a rate of 100 °C/h and stayed for 6h and then cooled to 900 °C with the rate 3°C/h. Crystals were extracted by etching in diluted HCl acid. The stoichiometry of a representative crystal was confirmed by semiquantitative energy-dispersive x-ray (EDX) microanalysis. Zero field cooled (ZFC) and field cooled (FC) magnetic susceptibility ( $\chi$ ) as a function of temperature was measured using a commercial Quantum Design SQUID magnetometer with field applied along the  $c$  direction ( $H\parallel c$ ) and in the  $ab$  plane ( $H\parallel ab$ ) of the crystal. Temperature dependent  $\rho(T)$  and  $C_p(T)$  measurements were performed using a Quantum Design Physical Property Measurement System (PPMS) for  $H\parallel ab$  only. All the above measurements were carried out down to 1.8 K except that  $C_p(T)$  was measured down to 0.37 K by using an additional  $^3\text{He}$  cooling system. The NMR measurements were carried out using the conventional pulsed NMR technique on  $^{75}\text{As}$  (nuclear spin  $I = 3/2$  and gyromagnetic ratio  $\gamma/2\pi = 7.2914$  MHz/T) nuclei in a temperature range  $4\text{ K} \leq T \leq 160\text{ K}$ . The measurements were done at a radio frequency of 48 MHz in single crystals with external magnetic field  $H$  applied along the  $c$  direction ( $H\parallel c$ ) and within the plane ( $H\parallel ab$ ). For this purpose we have taken five single crystals and glued them on top of each other to make a stack of single crystals. The field sweep NMR spectra were obtained by integrating the spin-echo in the time domain and plotting the resulting intensity as a function of the field. The spin lattice relaxation rate ( $1/T_1$ ) measurements were also performed at 48 MHz in both the field directions ( $H\parallel c$  and  $H\parallel ab$ ) following the standard saturation recovery method by exciting the central transition of  $^{75}\text{As}$  spectra.

## 3. Results and Discussion

### 3.1. Electrical Resistivity, Magnetic Susceptibility and Specific Heat

The results of the electrical resistivity normalized by the room temperature value ( $\rho/\rho_{300\text{K}}(T)$ ) as a function of temperature is presented in Fig. 1 for  $(\text{Eu}_{0.2}\text{Sr}_{0.8})\text{Fe}_2\text{As}_2$  and ESFCA crystals.  $\rho(T)$  for  $(\text{Eu}_{0.2}\text{Sr}_{0.8})\text{Fe}_2\text{As}_2$  is weakly temperature dependent at high temperatures, shows a broad hump at  $T \simeq 210\text{ K}$ , and then decreases almost linearly with decrease in temperature for  $T < 210\text{ K}$  before it attains a saturation value at  $T \leq 20\text{ K}$ . The broad hump at 210 K is an indication of the SDW transition which is about 15 K higher than the transition temperature reported for the parent compound  $\text{EuFe}_2\text{As}_2$  [12]. The linear decrease of  $\rho(T)$  points towards the metallic nature of the

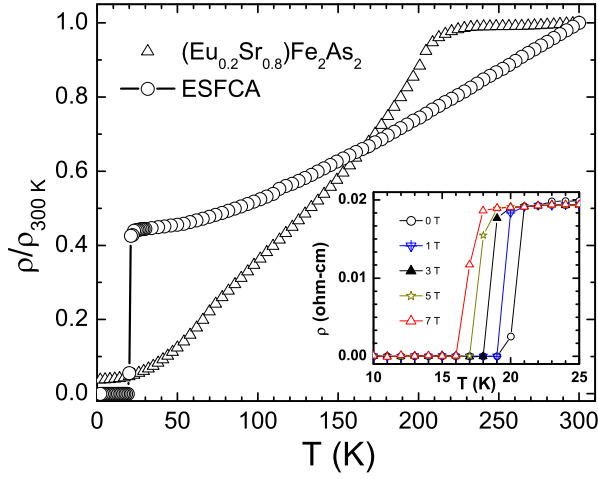


**Figure 1.** Temperature dependence of electrical resistivity  $\rho(T)$  of  $\text{Eu}_{0.2}\text{Sr}_{0.8}\text{Fe}_2\text{As}_2$  and superconducting ESFCA single crystals. Inset shows the low temperature  $\rho(T)$  measured at different applied fields to highlight the  $T_C$  of ESFCA.

compound. No trace of superconductivity or  $\text{Eu}^{2+}$  ordering was found down to 2 K suggesting that the  $\text{Eu}^{2+}$  ordering at 19 K reported for  $\text{EuFe}_2\text{As}_2$  is suppressed below 2 K after 80% Sr doping at the Eu site. The overall behaviour of  $\rho(T)$  is identical to the previous report on the parent compound  $\text{EuFe}_2\text{As}_2$ [12] except that the SDW transition temperature is enhanced and the  $\text{Eu}^{2+}$  ordering is suppressed. At 300 K and 2 K the values of  $\rho$  are about 16 m $\Omega$ -cm and 0.59 m $\Omega$ -cm, respectively yielding a residual resistivity ratio ( $\rho_{300\text{ K}}/\rho_{2\text{ K}}$ ) of 27. Such a high value of  $\rho_{300\text{ K}}/\rho_{2\text{ K}}$  is indicative of a high quality sample with only small amount of disorder present in the material. As shown in Fig. 1 for 14% Co substitution at the Fe site, the SDW transition is suppressed completely, and  $\rho$  shows a linear decrease with temperature down to 25 K. At  $T \simeq 22$  K,  $\rho(T)$  drops abruptly and reaches zero value by 20 K due to the onset of superconductivity. The low- $T$  part of  $\rho(T)$  measured at various applied fields ( $H$ ) is plotted in the inset of Fig. 1 to highlight the variation of superconducting transition temperature ( $T_C$ ) with  $H$ . As the field  $H$  increases, the  $T_C$  decreases gradually.

Beside the transport measurements magnetic measurements are performed to probe the superconducting transition. Figure 2 shows the ZFC and FC dc susceptibility for the two directions. The field applied is 0.002 T and  $\chi(T)$  is plotted in units of  $4\pi\chi_v$  where  $\chi_v = -1/4\pi$  indicate complete diamagnetic behaviour. The superconducting transition at about 20 K is confirmed by the ZFC signal. Here  $\chi_v$  for  $T \rightarrow 0$  is strongly enhanced for the  $H\parallel c$  direction which could be assigned to the demagnetization effect. Furthermore the finite size of the crystal in relation to the superconducting penetration depth also influence the magnetization. The  $a$  and  $b$  dimension are larger than the  $c$  dimension which strongly increases the demagnetization factor resulting to an enhanced

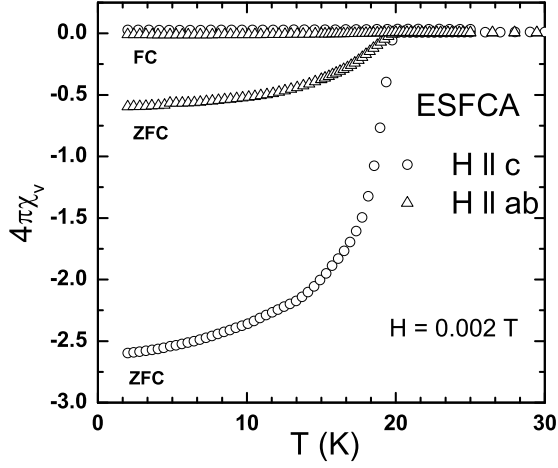


**Figure 2.** Temperature dependence of ZFC and FC magnetic susceptibility of single crystalline ESFCA measured at an applied field of 0.002 T along two orientations.

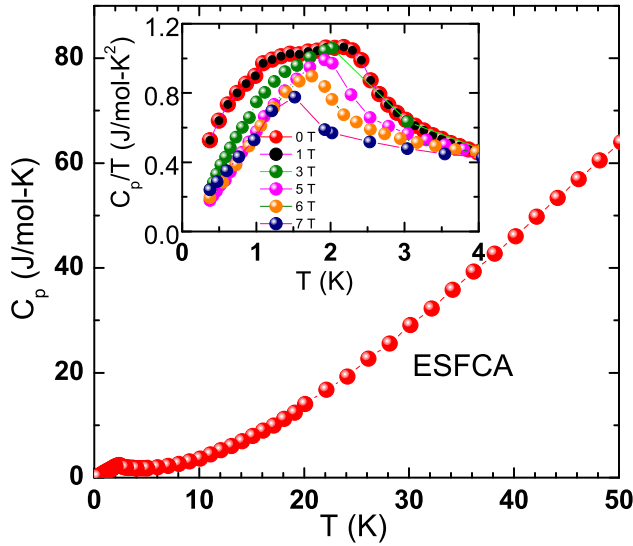


**Figure 3.** Temperature dependence of the heat capacity  $C_p$  of ESFCA. Inset shows  $C_p/T$  vs.  $T$  measured at different fields in the low temperature regime.

magnetization for that direction. Down to 1.8 K, no signature of  $\text{Eu}^{2+}$  ordering was observed in the ZFC and FC  $\chi(T)$  measurements. Nevertheless an AFM transition superimposed by a large response from a superconducting transition is not easy to resolve in the SQUID.

As a final proof we carried out specific heat measurements on single crystals, to

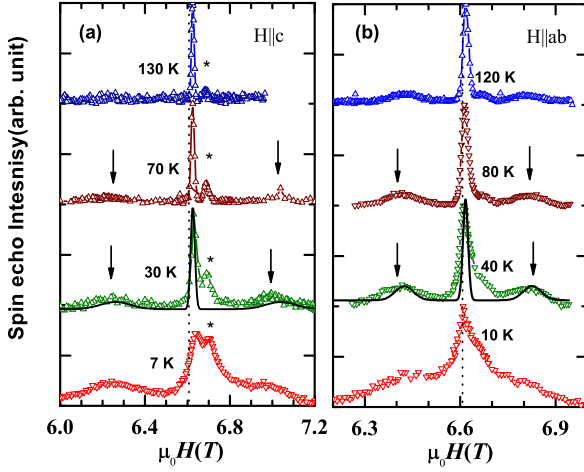


**Figure 4.**  $^{75}\text{As}$  field sweep spectra of ESFCA measured at various temperatures with external field applied parallel to the (a)  $c$ -direction ( $\text{H}\parallel c$ ) and (b)  $ab$ -plane ( $\text{H}\parallel ab$ ). The down arrows exhibit the satellite transitions ( $\pm 1/2 \leftrightarrow \pm 3/2$ ) and the solid lines are the theoretical fits with the parameters given in the text. The star mark points to the extra peak close to the central line for  $\text{H}\parallel c$ . Dotted vertical lines indicate the position of the Larmor field.

check whether there exists the heat capacity jump associate with  $T_C$  and how far the  $\text{Eu}^{2+}$  ordering is suppressed, over the temperature range  $0.37 \leq T \leq 50$  K. Figure 3 shows the  $C_p(T)$  data measured at zero field. The SC transition is not visible because the small jump of  $\Delta C_{\text{SC}} \simeq 0.8$  J/mol-K at  $T_c \simeq 20$  K could not be easy to extract from the phonon dominate specific heat[13]. Nonetheless the magnetic ordering of  $\text{Eu}^{2+}$  could be clearly identified. A sharp anomaly however was observed at about 2 K which can be attributed to the  $\text{Eu}^{2+}$  ordering ( $T_N$ ). To understand the nature of the magnetic ordering we measured  $C_p(T)$  at different applied fields upto 7 T in the low- $T$  regime and  $C_p/T$  vs.  $T$  is presented in the inset of Fig. 3. With increase in field the height of the anomaly decreases and  $T_N$  was found to move towards low temperatures as is expected for an AFM ordering. Furthermore integrating  $C_p/T$  over temperature range 0.37-6 K associated with the anomaly reveals an entropy gain  $\Delta S=4$ , which is 23% of  $R\ln 8$ .

### 3.2. $^{75}\text{As}$ NMR

$^{75}\text{As}$ -NMR measurements are performed on the two different crystallographic directions ( $\text{H}\parallel c$  and  $\text{H}\parallel ab$ ).  $^{75}\text{As}$ -field sweep NMR spectra are shown in Fig. 4. For both configurations, along with the most intense central line the spectrum contains extra shoulder-like features on either side.  $^{75}\text{As}$  has an electric quadrupolar moment that interacts with the local electric field gradient (EFG) in the crystal giving rise to the splitting of the NMR line. Therefore in principle, in case of lower crystal symmetry system (for example tetragonal and orthorhombic symmetry), one should see in the  $^{75}\text{As}$

spectra three allowed transitions:  $I_z = -1/2 \longleftrightarrow +1/2$  central transition, and the two  $I_z = \pm 1/2 \longleftrightarrow \pm 3/2$  satellite transitions. Thus the extra shoulders in the experimental spectra correspond to the first order splitting satellite transitions as indicated by the downward arrows in Fig. 4. In an attempt to fit the experimental spectra taking into account both the EFG and the Knight shift effects in different axes, we find that the spectra 30 K ( $\text{H} \parallel c$ ) and 40 K ( $\text{H} \parallel ab$ ) can be fitted reasonably well with the parameters (Knight-shift  $K_c \simeq -0.55\%$ , quadrupolar frequency  $\nu_Q \simeq 2.82$  MHz, width of central peak  $\simeq 145$  kHz, width of satellite  $\simeq 1050$  kHz, and EFG asymmetry parameter  $\eta \simeq 0$ ) and ( $K_{a,b} \simeq -0.321\%$ ,  $\nu_Q \simeq 1.47$  MHz, width of central peak  $\simeq 228.55$  kHz, width of satellite  $\simeq 600$  kHz, and  $\eta \simeq 0$ ), respectively (see Fig. 4) These  $\nu_Q$  values are slightly higher than that reported for single crystalline  $\text{SrFe}_2\text{As}_2$  compound [30]. The central line position is found to be almost temperature independent or shifting very weakly. At low temperatures, the NMR line is found to be broaden abruptly. As seen from the  $C_p(T)$  measurements  $\text{Eu}^{2+}$  orders antiferromagnetically below 2 K. Thus our NMR line broadening possibly arising due to the persistent magnetic correlation while approaching the  $\text{Eu}^{2+}$  ordering.

Rather broad satellite transitions are observed in comparison to the sharp central transition indicating a distribution of EFG. Due to the doping of Sr and Co, the disorderness has been inevitably introduced in this system, resulting a rather distribution of EFG. In Fig. 4(a) apart from the central and satellite transition another small peak is observed at around 6.65 T (assigned as \*). The small peak is originated because of the substitution of 14% Co at the Fe site which essentially modify the As neighbors [25]. By lowering the temperature the central transition and the line marked by the \*, broadens and shifted concurrently to some equal extent. This perhaps indicates that As in the midst of different nearest neighbors have sensed the same magnetism. The perceptible line broadening could be described by two possibilities. First with lowering of the temperature the inevitable disorderness of this alloy have sponsored some additional line broadening and the second one could be associated with  $\text{Eu}^{2+}$  AFM ordering at low temperature. Nevertheless, the second argument is more likely as this supports field dependent specific heat scenario. Usually when a system is approaching towards the (AFM/FM) long range ordering due to the development of internal field associated with the magnetism the spectra broadens. Being a local probe NMR can sense this effect well above the ordering.

Spin-lattice relaxation rate  $1/T_1$  was measured by saturating the central line in the two field directions i.e.  $\text{H} \parallel c$  and  $\text{H} \parallel ab$  by the standard saturation recovery method. The recovery curves could be fitted consistently with single  $T_1$  component using the following equation down to 18 K,

$$1 - \frac{M(t)}{M(\infty)} = 0.1e^{-t/T_1} + 0.9e^{-6t/T_1}, \quad (1)$$

where  $M(t)$  is the nuclear magnetization at a time  $t$  after the saturation pulse and  $M(\infty)$  is the equilibrium magnetization. For  $T < 18$  K, another short  $T_1$  component is required to fit the recovery curves. As seen from Fig. 4, the extra peak close to the

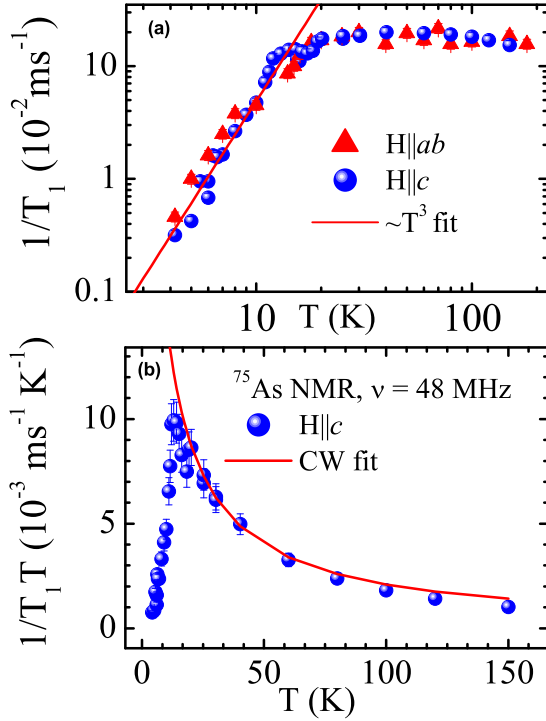


**Figure 5.** (a) Temperature dependence of the  $1/T_1$  for two external field directions  $H \parallel ab$  and  $H \parallel c$ . The solid line represents the  $T^3$  behaviour. (b)  $1/T_1 T$  as a function of temperature. The solid line exhibits Curie-Weiss fit  $\frac{C}{T+\theta}$ .

central line become more pronounce at low temperatures. Since  $1/T_1$  was measured at the central line position, we possibly saturate a fraction of that extra peak which is having a short  $T_1$  component. Another possibility could be the low temperature  $\text{Eu}^{2+}$  AFM ordering. The temperature dependence of  $1/T_1$  is presented in Fig. 5 measured for  $H \parallel ab$  and  $H \parallel c$  directions. For both the directions, the over all behaviour and magnitude of  $1/T_1(T)$  almost remains same. This indicates there is no significant anisotropy in the spin dynamics. At high- $T$ s,  $1/T_1$  is almost  $T$ -independent. With decrease in  $T$  ( $T \lesssim 18 \text{ K}$ ),  $1/T_1$  shows a gradual decrease without showing Hebel-Slichter coherence peak, benchmark for the  $s$ -wave type superconductivity. Here it is important to mention that the absence of Hebel-Slichter peak could be because of the extended  $s$ -wave scenarios, to which  $s_{\pm}$  state also belongs [31]. The change of slope in  $1/T_1$  at  $T \simeq 18 \text{ K}$  is likely due to the onset of superconductivity and is consistent with the  $\rho(T)$  data at  $H=7 \text{ T}$  which exhibit a sharp drop nearly at the same temperature (see Fig. 1). In the superconductive regime ( $T \leq 15 \text{ K}$ ),  $1/T_1$  follows a  $T^3$  behavior. This possibly is an indication of non  $s$ -wave type superconductivity and/or line nodes in superconductivity gap.

The nuclear spin-lattice relaxation rate,  $\frac{1}{T_1}$ , is related to the dynamic susceptibility



$\chi_M(\vec{q}, \omega_0)$  per mole of electronic spins[32, 33] as

$$\frac{1}{T_1 T} = \frac{2\gamma_N^2 k_B}{N_A^2} \sum_{\vec{q}} |A(\vec{q})|^2 \frac{\chi_M''(\vec{q}, \omega_0)}{\omega_0}, \quad (2)$$

where the sum is over wave vectors  $\vec{q}$  within the first Brillouin zone,  $A(\vec{q})$  is the form factor of the hyperfine interactions as a function of  $\vec{q}$  in units of  $\text{Oe}/\mu_B$ , and  $\chi_M''(\vec{q}, \omega_0)$  is the imaginary part of the dynamic susceptibility at the nuclear Larmor frequency  $\omega_0$  in units of  $\mu_B/\text{Oe}$ . The uniform static molar susceptibility  $\chi = \chi_M'(0, 0)$  corresponds to the real component  $\chi_M'(\vec{q}, \omega_0)$  with  $q = 0$  and  $\omega_0 = 0$ . According to the mean-field theory, when the relaxation process is dominated by the two-dimensional(2D) and three dimensional(3D) AFM fluctuations, Eq. 2 reduces to  $\frac{1}{T_1 T} \sim \frac{C}{T+\theta}$  (Curie-Weiss law) and  $\frac{1}{T_1 T} \sim \frac{C}{(T+\theta)^{0.5}}$ , respectively.[32] In the Fig.5(b), we have plotted  $1/T_1 T$  vs.  $T$ . It increases with decrease in temperature down to 18 K following a Curie-Weiss (CW) law  $1/T_1 T = \frac{C}{T+\theta}$  in the temperature range  $18 \text{ K} \leq 150 \text{ K}$ . The solid line shows the CW fit with parameters  $C \simeq 0.22 \text{ (ms)}^{-1}$ , and Weiss temperature  $\theta \simeq 5 \text{ K}$ . We interpret this feature as arising from two dimensional AFM fluctuations.

The positive Weiss temperature indicates that SC is observed with the complete suppression of magnetic order. This scenario is similar to the case of  $\text{LaFeAs}(\text{O}_{1-x}\text{F}_x)$ , F doped system where Nakai et. al. observed the positive Weiss temperature [34] and has been predicted that the SC emerges when a magnetic ordering is suppressed. This tendency is similar to that in  $1/T_1 T$  of Cu in underdoped  $\text{La}_{2-x}\text{Sr}_x\text{CuO}_4$ , [35] where superconductivity also observed with a positive Weiss temperature.

#### 4. Conclusions

The presented results point to a bulk SC with a transition at  $T_C=20 \text{ K}$  at zero field. With field the  $T_C$  is shifted towards lower temperature. The field dependent  $C_p/T$  study suggests the AFM ordering of  $\text{Eu}^{2+}$  moment at  $T_N=2 \text{ K}$ . This AFM ordering is shifted towards lower temperature from 19 K due to the  $\text{Sr}^{2+}$  substitution at the  $\text{Eu}^{2+}$  site in  $\text{EuFe}_2\text{As}_2$ .

In order to get a deeper microscopic insight we have performed  $^{75}\text{As}$  NMR investigations on single crystals of ESFCA in the external field  $H\parallel c$  and  $H\parallel ab$  directions.  $^{75}\text{As}$  field sweep NMR spectra broadens with lowering the temperature and the obtained value of  $\nu_Q$  is somewhat higher than that has been obtained for  $\text{SrFe}_2\text{As}_2$  single crystals. This line broadening phenomena is associated with the low temperature  $\text{Eu}^{2+}$  AFM ordering and could be to some extent due to the disorder. The spin-lattice relaxation rate  $1/T_1$  results in the two crystallographic directions indicate the absence of substantial anisotropy in the spin dynamics. The temperature dependence of  $1/T_1$  exhibits decrement below the SC transition following a  $T^3$  behaviour without any Hebel-Slichter coherence peak. This feature indicates the non s wave type SC and possibly could be explained within the framework of  $s_{\pm}$  model with impurity effect[36]. Moreover, the strong increase of  $1/T_1 T$  following CW law arising from two dimensional

AFM fluctuations.

NMR line broadening gives the supportive evidence of  $\text{Eu}^{2+}$  AFM ordering. On the other hand the drop of  $1/T_1$  following a  $T^3$  behaviour below 18 K is a signature of bulk SC. To illuminate this picture one could have possibly consider the coupling between the  $\text{Eu}^{2+}$  moment and the SC. Essentially  $\text{Eu}^{2+}$  moment polarizes the conduction electrons (CE), and they are coupled with the  $^{75}\text{As}$  nuclei via the Fermi contact interaction, as a result, the line broadening showed up in the  $^{75}\text{As}$  NMR spectra. On the other hand  $T_1$  is the measure of low energy electronic spin fluctuations and in the SC arena this is modified by the electron pairing. Therefore there is a possibility of coupling between the SC and the  $\text{Eu}^{2+}$  magnetism. Furthermore it is important to mention that at  $T > 20$  K nearly  $T$ -independent behaviour of  $1/T_1$  is observed in both directions. This constant  $1/T_1$  value possibly indicates,  $1/T_1$  is dominated by the relaxation process to the spin fluctuations of localized  $\text{Eu}^{2+}$  moments [37].

## Acknowledgments

RN would like to acknowledge MPG and DST India for financial support through MPG-DST fellowship. Work at Göttingen University is supported by DFG-SPP 1458.

## References

- [1] Kamihara Y, Watanabe T, Hirano M and Hosono H 2008 *J. Am. Chem. Soc.* **130**, 3296
- [2] Chen X H, Wu T, Wu G, Liu R H, Chen H, Fang D F 2008 *Nature* **453**, 1224
- [3] Ren Z A, Yang J, Lu W, Yi W, Che G C, Dong X L, Sun L L and Zhao Z X 2008 *Mater. Res. Innovations* **12**, 105
- [4] Chen G F, Li Z, Wu D, Li G, Hu W Z, Dong J, Zheng P, Luo J L and Wang N L 2008 *Phys. Rev. Lett.* **100**, 247002
- [5] Yang J, Li Z C, Lu W, Yi W, Shen X L, Ren Z A, Che G C, Dong X L, Sun L L, Zhou F and Zhao Z X 2008 *Supercond. Sci. Technol.* **21**, 082001
- [6] Bos J G, Penny G B S, Rodgers J A, Sokolov D A, Huxley A D and Attfield A P 2008 *Chem. Commun. (Cambridge)* **31**, 3634
- [7] Rotter M, Tegel M and Johrendt D 2008 *Phys. Rev. Lett.* **101**, 107006
- [8] Jeevan H S, Hossain Z, Kasinathan D, Rosner H, Geibel C and Gegenwart P 2008 *Phys. Rev. B* **78**, 092406
- [9] Sefat A S, Jin R, McGuire M A, Sales B C, Singh D J and Mandrus D 2008 *Phys. Rev. Lett.* **101**, 117004
- [10] Leithe-Jasper A, Schnelle W, Geibel C and Rosner H 2008 *Phys. Rev. Lett.* **101**, 207004
- [11] Raffius H, Morsen M, Mosel B D, Mller-Warmuth W, Jeitschko W, Terbchte L and Vomhof T 1993 *J. Phys. Chem. Solids* **54**, 135
- [12] Jeevan H S, Hossain Z, Kasinathan D, Rosner H, Geibel C and Gegenwart P 2008 *Phys. Rev. B* **78**, 052502
- [13] Zaanen J 2009 *Phys. Rev. B* **80**, 212502
- [14] Wu D, Barisic N, Drichko N, Kaiser S, Faridian A, Dressel M, Jiang S, Ren Z, Li L J, Cao G H, Xu Z A, Jeevan H S and Gegenwart P 2009 *Phys. Rev. B* **79**, 155103
- [15] Ren Z, Tao Q, Jiang S, Feng C, Wang C, Dai J, Cao G and Xu Z 2009 *Phys. Rev. Lett.* **102**, 137002
- [16] Jeevan H S, Kasinathan D, Rosner H and Gegenwart P 2011 *Phys. Rev. B* **83**, 054511

- [17] Miclea C F, Nicklas M, Jeevan H S, Kasinathan D, Hossain Z, Rosner H, Gegenwart P, Geibel C and Steglich F 2009 *Phys. Rev. B* **79**, 212509
- [18] Nicklas M, Kumar M, Lengyel E, Schnelle W and Leithe-Jasper A 2011 *J. Phys.: Conf. Ser.* **273**, 012101
- [19] Zheng Q, He Y, Wu T, Wu G, Chen H, Ying J, Liu R, Wang X, Xie Y, Yan Y, Li Q and Chen X 2009 arXiv:0907.5547
- [20] Hu R, Budko S L, Straszheim W E and Canfield P C 2011 *Phys. Rev. B* **83**, 094520
- [21] Ren Z, Lin X, Tao Q, Jiang S, Zhu Z, Wang C, Cao G and Xu Z 2009 *Phys. Rev. B* **79**, 094426
- [22] Jiang S, Luo Y, Ren Z, Zhu Z, Wang C, Xu X, Tao Q, Cao G and Xu Z 2009 *New Journal of Physics* **11**, 025007
- [23] Dengler E, Deisenhofer J, Krug von Nidda H A, Khim S, Kim J S, Kim K H, Casper F, Felser C and Loidl A 2010 *Phys. Rev. B* **81**, 024406
- [24] Ning F L, Ahilan K, Imai T, Sefat A S, Jin R, McGuire M A, Sales B C and Mandrus D 2009 *Phys. Rev. B* **79**, 140506(R)
- [25] Ning F L, Ahilan K, Imai T, Sefat A S, McGuire M A, and Sales B C, Mandrus D, Cheng P, Shen B and Wen H H 2010 *Phys. Rev. Lett.* **104**, 037001
- [26] Laplace Y, Bobroff J, Rullier-Albenque F, Colson D and Forget A 2009 *Phys. Rev. B* **80**, 140501
- [27] Baek S H, Lee H, Brown S E, Curro N J, Bauer E D, Ronning F, Park T and Thompson J D 2009 *Phys. Rev. Lett.* **102**, 227601
- [28] Kitagawa K, Katayama N, Gotou H, Yagi T, Ohgushi K, Matsumoto T, Uwatoko Y and Takigawa M 2009 *Phys. Rev. Lett.* **103**, 257002
- [29] Guguchia Z, Roos J, Shengelaya A, Katrych S, Bukowski Z, Weyeneth S, Muranyi F, Strässle S, Maisuradze A, Karpinski J and Keller H 2011 *Phys. Rev. B* **83**, 144516
- [30] Kitagawa K, Katayama N, Ohgushi K and Takigawa M 2009 *J. Phys. Soc. Jpn.* **78**, 063706
- [31] Parker D, Dolgov O V, Korshunov M M, Golubov A A and Mazin I I 2008 *Phys. Rev. B* **78**, 134524
- [32] Johnston D C 2010 *Advances in Phys.* **59**, 803
- [33] Moriya T 1963 *J. Phys. Soc. Jpn.* **18**, 516
- [34] Nakai Y, Ishida K, Kamihara Y, Hirano M, and Hosono H 2008 *J. Phys. Soc. Jpn.* **77**, 073701
- [35] Ohsugi S, Kitaoka Y, Ishida K and Asayama K 1991 *J. Phys. Soc. Jpn.* **60**, 2351
- [36] Ishida K, Nakai Y and Hosono H 2009 *J. Phys. Soc. Jpn.* **78**, 062001
- [37] Yamamoto A, Iemura S, Wada S, Ishida K, Shirogami I and Sekine C 2008 *J. Phys.: Condens. Matter* **20**, 195214